ORIGINAL ARTICLE

Synthesize and Characterize the Lipoid S-75 Conjugated Chitosan-Based Micelles for Improving Biopharmaceutical Parameters of Resveratrol

Mrunal Deshmukh[1], Geeta Kalyankar[2]

[1]Department of Pharmaceutics, Datta Meghe College of Pharmacy, DMIHER (DU), Swangi (Meghe), Wardha, Maharashtra, India, [2]Department of Pharmaceutics, Rajrashi Shahu College of Pharmacy, Buldhana, Maharashtra, India

Abstract

The anticancer activity of resveratrol is well known. But because of its limited water solubility and low bioavailability, resveratrol (RES) is a BCS class II medication with research potential. The current work creates a new copolymer from Lipoid S-75 and chitosan and tests the RES-loaded micelles it produces for varied delivery properties. In addition to efficiently loading the drug, the nanometric micellar carriers also regulated the rate of RES release. The discoveries using a novel polymer-based carrier show promise for improved medication delivery in the future. **Aim:** The aim of the study was to synthesize and characterize the lipoid S-75 conjugated chitosan-based micelles for improving biopharmaceutical parameters of resveratrol. **Methods:** The preparation and characterization of a copolymer of CS and lipoid S-75 were done by using S-75 100 mg and DCC 700 mg which is followed by preparation and characterization of CS-lipoid S-75-conjugated resveratrol micelles. And evaluation of the formulation done by the parameters such as particle size, polydispersity index zeta potential, % encapsulation efficiency and drug loading, drug loading capacity, and differential scanning calorimetry. **Results:** In the present study, development of polymeric micelles using the flavonoid in multifaceted applications, entailing therapy, diagnostics, in-suit imaging, and on-demand drug delivery, resveratrol, polymers such as chitosan, and lipoid S-75 show significant potential. The fundamental formation mechanisms are then analyzed, focusing on the inherent physicochemical qualities like solubility and bioavailability that control the drug release. **Conclusion:** The development of resveratrol-loaded chitosan-based S-75 micelles demonstrates considerable potential for multifaceted biomedical applications, including therapy, diagnostics, in-situ imaging, and on-demand drug delivery. The combination of resveratrol, chitosan, and lipoid S-75 results in a polymeric micellar system with enhanced solubility and bioavailability, addressing the challenges associated with the poor aqueous solubility and rapid metabolism of resveratrol. The analysis of the micelle formation mechanisms highlights the crucial role of the inherent physicochemical properties in controlling drug release. This innovative micellar platform offers promising avenues for optimizing the therapeutic delivery of resveratrol and broadening its application scope in pharmaceutical and biomedical fields.

Key words: Chitosan, lipoid S-75, polymeric micelles, resveratrol

INTRODUCTION

Flavonoids are polyphenolic substances essential secondary metabolites[1] and impart hue, flavor, and pharmacological characteristics to plants.[2] Flavonoids have attracted a wealth of interest and have undergone extensive clinical and laboratory examinations to explore whether they can aid in treating many acute and long-term health variables. Flavonoids are robust antioxidants that shield

Address for correspondence:
Mrunal Deshmukh, Datta Meghe College of Pharmacy, DMIHER (DU), Swangi (Meghe), Wardha - 442001, Maharashtra, India.
Phone: 8788711659/8805044235.
E-mail: mrunal.pharmacy@dmiher.edu.in

Received: 03-11-2024
Revised: 06-08-2024
Accepted: 21-08-2024

plants from detrimental climatic conditions.[3] Cultured and animal studies, flavonoids' immune modulation, anti-inflammatory, and profound anticancer effects have been shown.[4]

Resveratrol (3,5,4′-trihydroxystilbene), a stilbene found in substantial concentrations in peanuts, berries, grapes, other plant sources, and similarly in red wine, is a naturally occurring polyphenolic molecule.[5] This chemical has grown in popularity as a result of its anticancer properties, which were initially described in 1997.[6] Despite medical and technological advances over the past 20 years, cancer is still a major worldwide health problem.[7]

Herbs have been utilized to impact cellular signaling for years as either supplemental medicine or dietary agents. For example, resveratrol, a substance produced from grapes, has been used as a cancer treatment option. According to several studies, resveratrol has a wide variety of cancer-prevention and treatment alternatives. Furthermore, resveratrol has been generally regarded as having anticancer potential when paired with other chemotherapeutic medicines, and it has gotten a lot of interest for its prospect as a chemo preventive agent to combat human tumors. In a comparable direction, several researches have examined resveratrol's activity against cancer cells.[8]

Aluyen *et al*. looked into apoptosis of cells, antiproliferation, and anti-inflammation to further clarify the impact of resveratrol on several cancer cell types.[9] A review of resveratrol's several mechanisms of action, including signaling routes involving growth indicators and receptor-specific tyrosine kinases, growth factor-mediated signal transduction, cell death, and inflammation, was published by Varoni and colleagues in the identical vein.[10] These two publications emphasize on the workings of resveratrol toward a specific subset of malignancies, in contrast to other studies that concentrate on particular *in vitro* or *in vivo* research.[11]

The impact of resveratrol on hexokinase 2 (HK2) expressions and hepatocellular carcinoma (HCC) cell glycolysis was investigated by Dai *et al*. These researchers discovered that resveratrol therapy decreases cell growth in HCC cell lines in a dose-varying manner, due to glucose breakdown suppression in aerobic HCC cells. It also makes aerobic glycolytic HCC cells more sensitive.[12] Furthermore, after resveratrol therapy, mitochondrial apoptosis was associated to a considerable drop in HK2 expression.[13]

Resveratrol blocks action of phosphorylated liver kinase B1 on the aging of acute myeloid leukemia stem cells and induces apoptosis in CD34(+)CD38(−) KG1a cells via activating SIRT1, according to research by Yang *et al*. In addition, it activates caspase-3 and -9 in HepG2 cells, raises the Bax/Bcl-2 ratio, and results in p53 expression through cell death.[14] In addition, resveratrol (when paired with matrine) inhibits cell proliferation by (a) triggering cell death by activating caspase-3 and caspase-9, (b) restricting survivin, (c) generating reactive oxygen species (ROS), and (d) modifying the mitochondrial membrane potential.

Akin to this, it has anticancer effects on the hepatoma cell lines HepG2, Hep3B, and HuH7 and dose-dependently inhibits the activity of 11 human histone deacetylase enzymatic classes; I, II, and IV. In liver cancer cells, resveratrol increases transcription and mRNA stability, which incites MAT2B V1 and V2 expression in a way that varies with time and dose.[3] HuR expression rises after resveratrol therapy, which also affects SIRT1 and MAT2B. Similar to HuR, an RNA-binding protein, SIRT1 promotes MAT2B transcription while improving MAT2B mRNA stability.[15]

In addition, resveratrol lessens MAT's connections with MAT2 and increases MAT's connections to HuR and SIRT1. The interaction between SIRT1, MAT, and HuR enhances the stability of these proteins, but MAT reduces the Ki of MAT2 for S- adenosylmethionine. Resveratrol suppresses growth and encourages apoptosis by upregulating MAT2B and downregulating MAT2BV1. In addition, it has the identical effect on MAT2BV2 growth.[16]. Resveratrol therapy (50 mg/kg BW/day) significantly lowers myosin light chain kinase expression, encourages apoptotic death, and inhibits hepatic carcinogenesis in HCC rats generated by diethylnitrosamine (DENA).[17]

ROS are produced when resveratrol (20–80 moL/L) is applied to murine hepatocarcinoma Hepa 1–6 cells for 24–72 h. This inhibits cell growth and encourages apoptotic cell death. The use of resveratrol (50, 100, and 300 mg/kg) therapy can reverse DENA-induced changes in interleukin (IL-1), hepatic tumor necrosis factor-, and IL-6 levels and expression.[18] These results suggest that the chemotherapy preventive measures of resveratrol-mediated rat liver tumorigenesis are associated with modifications in pro-inflammatory cytokines.[19] According to earlier studies by Zhang *et al*., resveratrol decreases the development of the Vascular endothelial growth factor protein and mRNA, blocks the activation of nuclear factor-kappa B, and lowers microvessel density.[20]

Current restrictions on the use of RES as a pharmaceutical medication for commerce include, among other things, its limited bioavailability and quick metabolism. Due to its limited dissolution and poor bioavailability, RES's *in vivo* effects appear to be impacted in this way.[9]

30 µg/mL is its solubility level in water, which is low. Resveratrol is classified as a "Class II" chemical under the biopharmaceutical classification system because it exhibits a solubility-restricted penetration across biologic membranes.[13]

To address this problem, we need to prepare unique formulation strategy, that is, formation of polymeric mixed

micelles which can enhance the biopharmaceutical properties of RES. Micelles are the aggregation of colloidal particles with both hydrophilic and hydrophobic components.[21]

James William McBain of the University of Bristol did ground breaking work in this field.

Structure

- Micelles have a hydrophilic (water-loving) head, which means they attract water while repelling fat[22]
- Micelles feature hydrophobic (water-hating) tails that attract fat while repelling water[23]
- Polymeric micelles are nanoscale structures that range in size from 10 to 100 nanometers.[24]

METHODS

Preparation and characterization of a copolymer of CS and lipoid S-75

Synthesis of CS-S75 co-polymer

20 mL of de-ionized water and 1 mL of strong nitric acid were used to dissolve 100 mg of CS. S-75 100 mg and DCC 700 mg were mixed together in 10 mL of ethanol. The resultant ethanolic solution was swiftly poured into the CS solution while being continuously stirred for 5 min. The final product underwent 48 h of dialysis in comparison to 1000 mL of deionized water. The copolymer was created using the solvent evaporation technique by evaporating the residual solvent.

Critical Micellar concentration (CMC) determination

A well-known iodine technique was used to estimate the CMC values for the copolymer. An iodine standard solution was created by dissolving 500 mg of potassium iodide and 250 mg of iodine into 25 mL of de-ionized water. The copolymer was diluted in different amounts (1–16 g/mL), and 25 L of standard iodine solution was incorporated in successive dilutions. The resulting solutions were left in the absence of light for one night before they were analyzed with a Shimadzu ultraviolet (UV1800) UV-visible spectrophotometer. Plotting copolymer concentrations versus absorbance allowed us to calculate the CMC value. Absorbance increased noticeably at the CMC value.[24]

Fourier's transform infrared spectroscopy (FT-IR)

FTIR was used to investigate the structural characteristics of the produced copolymer and to identify the functional group present in materials.[25] Using an FT-IR spectrophotometer, the spectra of RES, CS, lipoid S-75, and CS-S-75 copolymer, RES-PM's and PM were collected across the range of 4000–400 cm^{-1} (Agilent Technologies 630 Cary).

PREPARATIONANDCHARACTERIZATION OF CS-LIPOID S-75-CONJUGATED RESVERATROL MICELLES

Preparation of CS-S-75 conjugated resveratrol micelles

In 2 mL of DMSO, 100 mg resveratrol and 200 mg CS-75 copolymer were dissolved. The solution was put in a syringe and drop-wise introduced into a beaker with ten milliliters of a phosphate-buffered saline solution (PBS 7.4) and 0.2% weight-by-weight Tween 80. To eliminate the remnants of organic solvent, the dispersion was sonicated in a water bath for 1 h and then dialysis against distilled water for 24 h. For future usage, the polymeric micelles were chilled. As a cryoprotectant, 2% w/w mannitol was added to the polymeric micelles before freezing. The powder was stored in a tightly sealed container for later use.[26]

Particle size, polydispersity index (PDI) zeta potential

Particle size, zeta potential, and PDI of RES-PMs were determined by Zetasizer Ver 6.0 (Malvern Instruments Ltd., Malvern). To achieve an acceptable scattering intensity, the material was diluted 1:10 with double distilled water before the tests. Each measurement was carried out three times. The analysis was done in a capillary cell at 25°C with a 90° detection angle. The PDI measures the RES-PMs population's size distribution. Droplet size analysis was performed after the sample was deposited in square glass cuvettes. In the absence of additional complicating elements like steric stabilizing agents or hydrophilic surface attachments, elevated levels of zeta potential may cause particles to disaggregate. The storage stability of colloidal dispersions can be predicted using zeta potential measurements.

% Encapsulation efficiency and drug loading

The encapsulation efficiency (%EE) can be determined by using following formula:

$$\% EE = W1/W2 \times 100$$

With W_1 being the weight of encapsulated drug;

W_2 is the total drug weight added in polymeric micelles formulation.

Drug loading capacity

The extent of dissolution betwixt the medicine and the polymer being used is what simply determines the drug-loading capacity. The Flory-Huggins interaction parameter can be used to predict whether a medicine and a polymer will work well together.[27] Drug-polymer is equal to (drug - polymer). 2 (RT/V drug) in which V drug is the molar

volume of the drug, drug and polymer are the Hildebrand-Scatchard solubility variables for the drug and the polymer, drug and polymer represent the interaction between the drug and the core-forming polymer, and T and R, are accordingly, the ideal gas constant and temperature.

Differential scanning calorimetry (DSC)

DSC thermograms were recorded for RES, CS, S-75, CS-S75 copolymer, and RES loaded CS-S75 polymeric micelles (RES-PM's) using DSC calorimeter (DSC 60, Shimadzu, Japan). The samples were scanned at a heating rate of 10°C/min, up to 250°C and a flow rate of 20 mL/min. under nitrogen atmosphere.

Sample dispatched for testing.

X-ray diffraction (XRD)

To compare the physical condition of resveratrol trapped in RES-PMs to that of free resveratrol, XRD examination was conducted. The spectrum was recorded using Cu K radiation (technically k1 and k2, with kβ eliminated by the primary optic), produced from a copper sealed tube X-ray source with a wavelength of 1.5406Å. It was used to analyze the XRD patterns of the drug (RES), CS, S-75, copolymer (CS-S75), and drug-co-polymer micelles (RES-PM's). The employment of a Göbel mirror optic produces a monochromatic parallel beam of X-ray energy (primary optic). For the purpose of capturing the diffracted X-rays, a set of protracted soller slits or parallel foils are positioned behind a scintillation counter detector. Although the sample is flat during the measurement, rotation can be used to enhance sampling and get rid of preferred orientation effects.

In vitro drug release studies

Weighed and sealed into dialysis bags (MWCO: 3500 Da), 1 mg of each of 100% RES and CS-S75 based RES-loaded polymeric micelles preparation. Using a USP dissolution device type-II kept at 37 ± 0.5°C, these bags were suspended in a 50 mL solution of PBS (pH 7.4) and ethanol (9:1 v/v ratio) at a paddle speed of 100 rpm. Periodically, 2 mL of the sample was removed and replaced with an equivalent fresh medium for sustaining the sink conditions. Collected samples were analyzed using UV-visible spectrophotometer at a wavelength of 307 nm (Shimadzu UV1800, Japan).

Transmission electron microscopy (TEM)

An optical microscope and the TEM are analogous. It has an astounding resolution, which may reach 0.1 nm for lattice images. Remarkably powerful magnification (almost 1 million times) is feasible. TEM can examine materials, replicas of sample surfaces, and micro sections (below 60-nm thickness) across cells and tissues.[28]

TEM analysis of RES-PMs was performed using a Hitachi (H-7500) 120 kV TEM with a charge-coupled device camera with a 40–120 kV working voltage, this instrument has a resolution of 0.36 nm (point to point) and can magnify objects up to 6 lakh times in high resolution mode. Electron diffraction, tungsten filament, low dose function, high contrast mode, and an ergo dynamic look are all present. Among the instrument's special characteristics (APIS) are the broadest possible views at ×700 with two picture options, auto-navigation, the largest field with the most remarkable contrast, and automated pre-irradiation mode. With the addition of electron energy loss spectroscopy, energy dispersive X-ray spectroscopy, and STEM attachments, the apparatus can eventually be transformed into an analytical system.

RESULTS AND DISCUSSION

Organoleptic properties

Table 1: Physical properties of resveratrol, chitosan

Sample	Appearance	Melting points (°C)	Solubility in water
Resveratrol	White powder with slight yellow cast	261–263	0.03 g/L
Chitosan	White	88–120	Insoluble in water

FT-IR

Identifying functional groups and their relationship with other chemicals utilized in formulations are crucial information that is obtained through FTIR studies. [Figure 1] shows the FTIR spectrum of resveratrol, lipoid S-75, RES-loaded CS-S75 copolymer, chitosan, resveratrol-loaded CS-S75 micelles, PM apiece. The FTIR spectrum of resveratrol [Figure 1a]. Betokens absorption acme at ~3168.2 (O-H stretching), 2922.2 (C-H stretching), 2359.4 (C=C=O stretching), 2117.1 (C≡C stretching), 1144.3 (C-O stretching). FTIR spectrum of lipoid S-75 [Figure 1b] reported absorption peaks at 3011.7 (O-H stretching), 2922.2 (C-H stretching), 1738.9 (C=O stretching), 1483.5 (C-H bending), 1319.5 (O-H bending), 1177 (C-O stretching), 1237.5 (C-O stretching). CS-S75 copolymer spectrum [Figure 1c] reported absorption peaks at 3324.8 (N-H stretching), 2926 (C-H stretching), 2851.4 (C-H stretching), 1625.1 (C=C stretching), 1438.8 (O-H bending), 1271.0 (C-O stretching). Chitosan spectrum [Figure 1d] reported absorption peaks at 3354.6 (O-H stretching), 2870.1 (C-H stretching), 1651.2 (N-H stretching), 1375.4 (O-H bending), 1021.3 (C-N stretching). RES loaded CS-S75

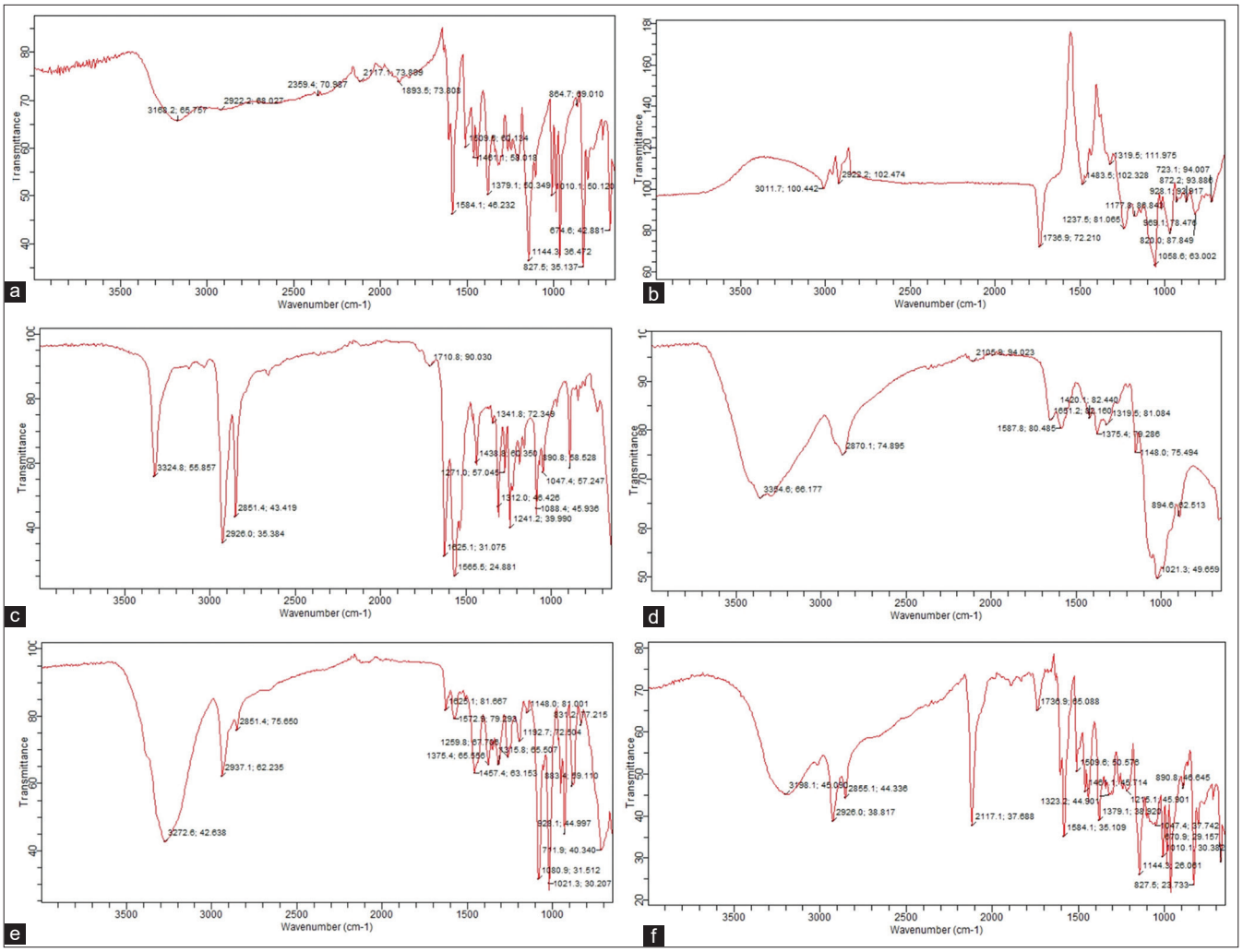

Figure 1: (a) Fourier's transform infrared spectroscopy (FTIR) spectrum of resveratrol. (b) FTIR spectrum of S-75. (c) FTIR spectrum of CS-S75 copolymer. (d) FTIR spectrum of chitosan. (e) FTIR spectrum of RES-PM's. (f) FTIR spectrum of physical mixture

micelles spectrum [Figure 1e] reported absorption peaks at 3272 (O-H stretching), 2937 (C-H stretching), 2851 (C-H stretching), 1625 (C=C stretching), 1457 (C-H bending), 1259 (C-O stretching). Physical mixture spectrum [Figure 1f] reported absorption peaks at 3198.1 (O-H stretching), 2926.0 (C-H stretching), 2855.1 (C-H stretching), 2117.1 (N=C=N stretching), 1736.9 (C=O stretching), 1584.1 (C=C stretching). The CMC value of prepared CS-S75 copolymer was observed as 0.00008 µg/mL by using iodine method [Figure 2].

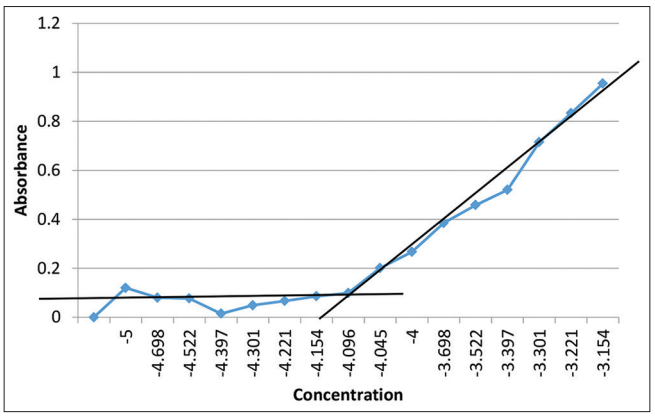

Figure 2: Critical micellar concentration of CS-S75 Copolymer

XRD pattern

Powder XRD (PXRD) is a unique characterization method that is commonly used to assess the crystalline state of a medication within a carrier matrix.[26] PXRD spectra of RES, CS, S-75, CS-S75 copolymer, RES-loaded CS-S75 micelles are shown in [Figure 3a-e] respectively. XRD pattern of resveratrol [Figure 3a] showed series of sharp intensity peaks indicates crystalline form of resveratrol. XRD pattern of chitosan [Figure 3b] showed series of two dissimilar, broad, and high-intensity peaks indicates amorphous as well as crystalline form of CS. XRD pattern of lipoid S-75 [Figure 3c] showed series of broad and high intensity peaks indicates polymorphic form. XRD pattern of CS-S75

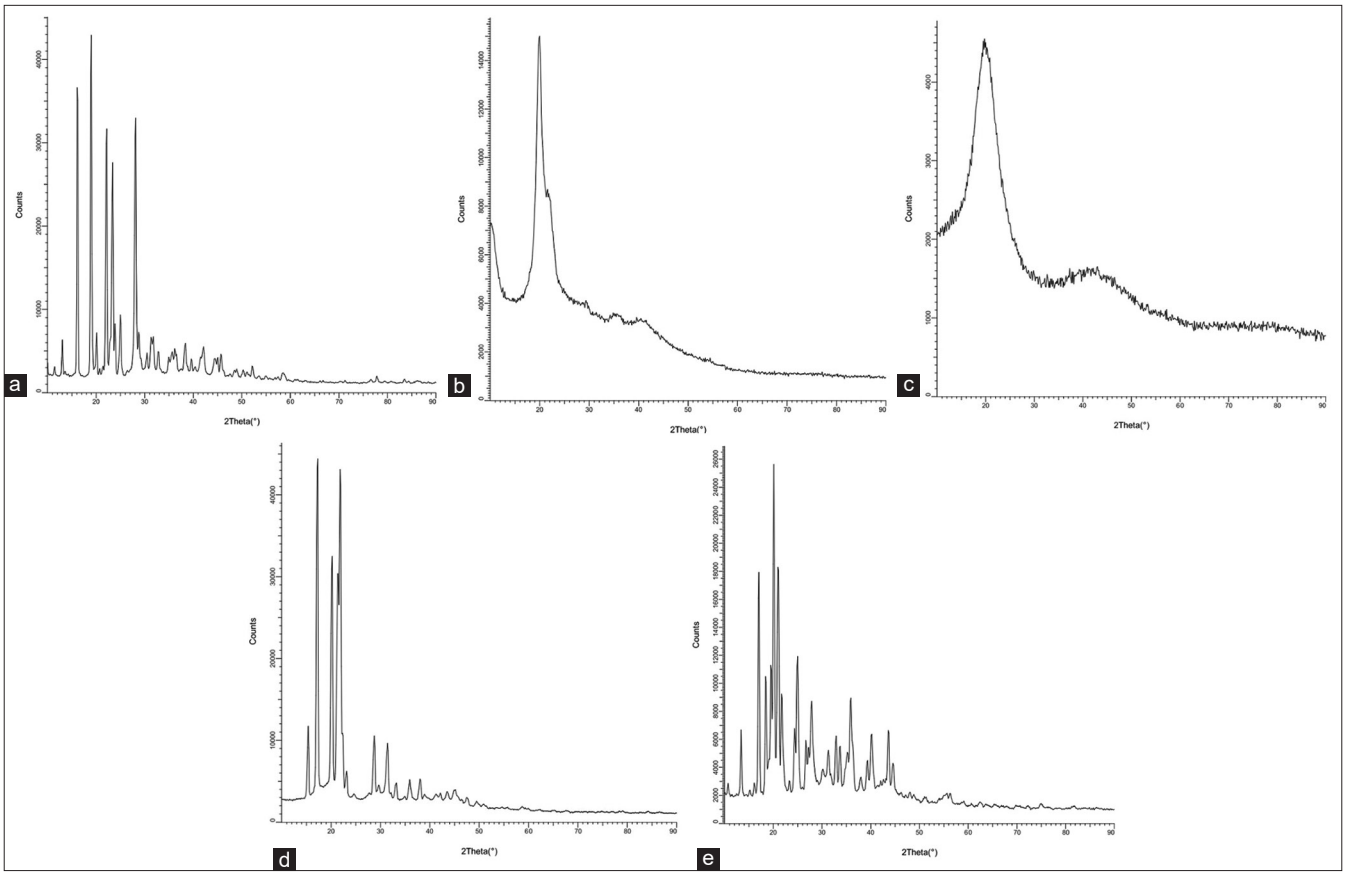

Figure 3: (a) X-ray diffraction (XRD) graph of resveratrol. (b) XRD graph of chitosan. (c) XRD graph of lipoid S-75. (d) XRD graph of CS-S75 copolymer. (e) XRD graph of RES loaded CS-S75 Micelles

copolymer [Figure 3d] showed sharp and a mixed intensity peak indicates polymorphic form. XRD pattern of RES-PM's [Figure 3e] showed less intense peak as compare to pure drug (RES) and it could be due to dispersion of RES within a polymer caused amorphization thereby RES-PM's shows less intense peak.

Particle, zeta potential, and PDI

The two key metrics used to assess the physical stability of sub-micron particulates in a liquid dispersion are variations in particle size and zeta potential. Disomin-phospholipids phytosomes with a particle size of 536 ± 3.66 nm were previously reported, and they were shown to be appropriate for oral administration due to their improved water solubility and oral bioavailability.[29] [Figure 4a] shows the particle size of RES-PM's was showed to ~291.9 (d.nm) as analyzed by Malvern. The PDI for RES-PM's turned out to be between 0.506, shown in [Table 1]. This value indicates the nanostructured nature of synthesized formulation. One of the critical characteristics of the particle, the zeta potential (ζ), controls the surface charges that surround the particles. In essence, it serves as a possible marker of the stability of the physical condition of the particles in a liquid dispersion.[30] The stability of colloidal dispersions with zeta potentials >25 mV has been documented.[31] [Figure 4b] shows the zeta potential of developed RES-PM's. In this work, zeta potential value for RES-PM's was observed to be −6.54 mV as evaluated by Malvern.

[Table 1] represents the %EE and %DL values of RES-PM's. The %EE value was 89%, while %DL value was 31%. The high % of EE value shows how effectively established methods can encapsulate pristine drugs. This may be due to the hydrophobic core of the RES-PMs that was adept at entrapping the hydrophobic drug inside of its core. As such, this copolymer enables considerable amounts of pure medication to be loaded in drug delivery applications.

Evaluation parameters of formulations

Formulation	RES-PM's
Drug polymer ratio	1:2
Particle size	~291.9 (d.nm)
PDI	~0.506
Zeta potential	–6.54 mV
Encapsulation efficiency (%)	89
Drug loading (%)	31

PDI: Polydispersity index, RES-PM's: Drug-co-polymer micelles

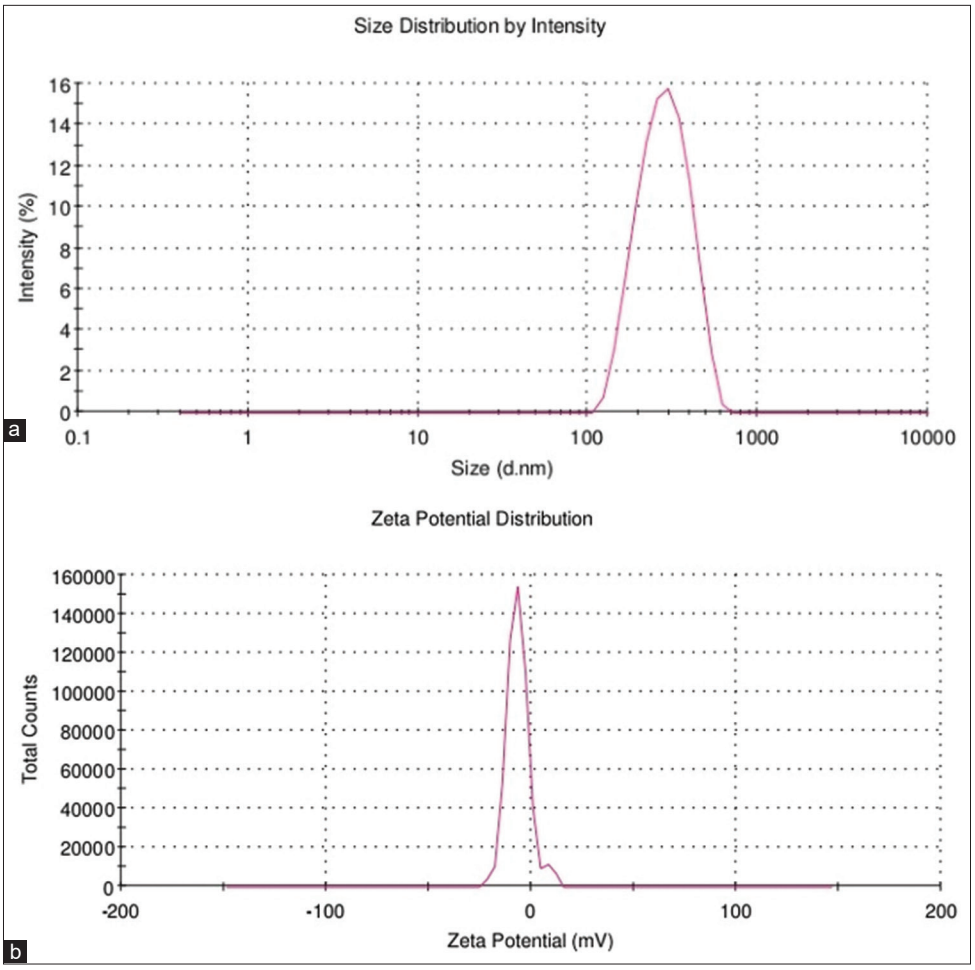

Figure 4: (a) Size distribution of formulation. (b) Zeta potential distribution of formulation

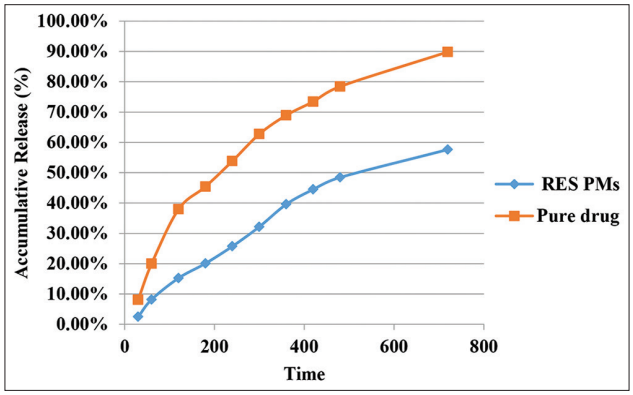

Figure 5: Drug release pattern of pure RES and RES-PMs

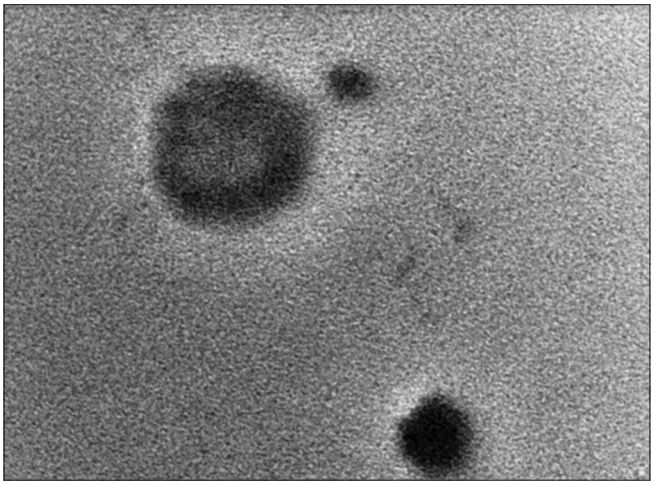

Figure 6: Transmission electron microscopy image of RES-PM's

In vitro drug release studies

Within 12 h of the research period, the dialysis technique in PBS (pH 7.4) was used to examine the cultured drug release trend of both pristine RES and RES-PM's formulation. Figure 5 shows a graph of percent cumulative drug release (CDR) (percent CDR) versus time.

As shown [Figure 5] RES showed sustained release behavior from RES-PM's. Up to 90% RES was release from pure RES within 12 h, while the release of RES from RES-PM's was release up to the 60% within 12 h. The results showed that core could accept the hydrophobic drug in a stable manner, resulting in regulated drug release.

TEM analysis

TEM micrograph of RES-PM's [Figure 6] evidenced to be in nanoscale range with round, nearly spherical shape. Outer

side of white round clearly indicates the shell structure and inner side of white round indicates the core structure. That means core and shell structure of micelles were developed.

SUMMARY AND CONCLUSION

In the present study, development of polymeric micelles using the flavonoid in multifaceted applications, entailing therapy, diagnostics, in-suit imaging, and on-demand drug delivery, resveratrol, polymers like chitosan, and lipoid S-75 show significant potential. Here, a brief overview of the resveratrol-loaded chitosan-based S-75 micelles is presented. The fundamental formation mechanisms are then analyzed, focusing on the inherent physicochemical qualities like solubility and bioavailability that control the drug release.

REFERENCES

1. Nabavi SM, Šamec D, Tomczyk M, Milella L, Russo D, Habtemariam S, *et al*. Flavonoid biosynthetic pathways in plants: Versatile targets for metabolic engineering. Biotechnol Adv 2020;38:107316.
2. Scarano A, Chieppa M, Santino A. Looking at flavonoid biodiversity in horticultural crops: A colored mine with nutritional benefits. Plants (Basel) 2018;7:98.
3. Vrhovsek U, Rigo A, Tonon D, Mattivi F. Quantitation of polyphenols in different apple varieties. J Agric Food Chem 2004;52:6532-8.
4. Rodríguez-García C, Sánchez-Quesada C, Gaforio JJ, Gaforio JJ. Dietary flavonoids as cancer chemopreventive agents: An updated review of human studies. Antioxidants (Basel) 2019;8:1-23.
5. Biesalski HK. Polyphenols and inflammation: Basic interactions. Curr Opin Clin Nutr Metab Care 2007;10:724-8.
6. Jang M, Cai L, Udeani GO, Slowing KV, Thomas CF, Beecher CW, *et al*. Cancer chemopreventive activity of resveratrol, a natural product derived from grapes. Science 1997;275:218-20.
7. Seyed MA, Jantan I, Bukhari SN, Vijayaraghavan K. A comprehensive review on the chemotherapeutic potential of piceatannol for cancer treatment, with mechanistic insights. J Agric Food Chem 2016;64:725-37.
8. Arts IC, Van De Putte B, Hollman PC. Catechin contents of foods commonly consumed in The Netherlands. 1. Fruits, vegetables, staple foods, and processed foods. J Agric Food Chem 2000;48:1746-51.
9 Aluyen JK, Ton QN, Tran T, Yang AE, Gottlieb HB, Bellanger RA. Resveratrol: Potential as anticancer agent. J Diet Suppl 2012;9:45-56.
10. Varoni EM, Fabrizio A, Faro L, Sharifi-rad J, Iriti M, Burd R, *et al*. Anticancer molecular mechanisms of resveratrol. 2016;3:8.
11. Liu J, Wang X, Yong H, Kan J, Jin C. Recent advances in flavonoid-grafted polysaccharides: Synthesis, structural characterization, bioactivities and potential applications. Int J Biol Macromol 2018;116:1011-25.
12. Kofink M, Papagiannopoulos M, Galensa R. (-)-Catechin in cocoa and chocolate: Occurence and analysis of an atypical flavan-3-ol enantiomer. Molecules 2007;12:1274-88.
13. Dai Z, Lei P, Xie JIE, Hu Y. Antitumor effect of resveratrol on chondrosarcoma cells via phosphoinositide 3-kinase/AKT and p38 mitogen-activated protein kinase pathways. Mol Med Rep 2015;12:3151-5.
14. Pandjaitan N, Howard LR, Morelock T, Gil MI. Antioxidant capacity and phenolic content of spinach as affected by genetics and maturation. J Agric Food Chem 2005;53:8618-23.
15. Wu X, Gu L, Prior RL, McKay S. Characterization of anthocyanins and proanthocyanidins in some cultivars of *Ribes*, *Aronia*, and *Sambucus* and their antioxidant capacity. J Agric Food Chem 2004;52:7846-56.
16. Yang H, Zheng Y, Li TW, Peng H, Fernandez-Ramos D, Martínez-Chantar ML, *et al*. Methionine adenosyltransferase 2B, HuR, and sirtuin. Protein cross-talk impacts on the effect of resveratrol on apoptosis and growth in liver cancer cells. J Biol Chem 2013;288:23161-70.
17. Zhang XL, Yu H, Xiong YY, Ma ST, Zhao L, She SF. Resveratrol down-regulates myosin light chain kinase, induces apoptosis and inhibits diethylnitrosamine-induced liver tumorigenesis in rats. Int J Mol Sci 2013;14:1940-51.
18. Slimestad R, Fossen T, Vågen IM. Onions: A source of unique dietary flavonoids. J Agric Food Chem 2007;55:10067-80.
19. Mbimba T, Awale P, Bhatia D, Geldenhuys WJ, Darvesh AS, Carroll RT, *et al*. Alteration of hepatic proinflammatory cytokines is involved in the resveratrol-mediated chemoprevention of chemically-induced hepatocar-cinogenesis. Curr Pharm Biotechnol 2012;2:229-34.
20. De Martel C, Ferlay J, Franceschi S, Vignat J, Bray F, Forman D, *et al*. Global burden of cancers attributable to infections in 2008: A review and synthetic analysis. Lancet Oncol 2012;13:607-15.
21. Walle T, Hsieh F, Delegge MH, Oatis JE Jr., Walle UK. High absorption but very low bioavailability of oral resveratrol in humans. Drug Metab Dispos 2004;32:1377-82.
22. Amri A, Chaumeil JC, Sfar S, Charrueau C. Administration of resveratrol: What formulation solutions to bioavailability limitations? J Control Release 2012;158:182-93.
23. Thipparaboina R, Chavan RB, Kumar D, Modugula S, Shastri NR. Colloids Sur B Biointerfaces 2015. doi: 10.1016/j.colsurfb.07.046,2015.
24. Thotakura N, Dadarwal M, Kumar R, Singh B, Sharma G, Kumar P, *et al*. Chitosan-palmitic acid based polymeric micelles as promising carrier for circumventing

pharmacokinetic and drug delivery concerns of tamoxifen. Int J Biol Macromol 2017;102:1220-5.
25. El-Feky GS, Sharaf SS, El Shafei A, Hegazy AA. Using chitosan nanoparticles as drug carriers for the development of a silver sulfadiazine wound dressing. Carbohydr Polym 2017;158:11-9.
26. Jones MC, Leroux JC. Polymeric micelles-a new generation of colloidal drug carriers. Eur J Pharm Biopharm 1999;48:101-11.
27. Hu F, Ren G, Yuan H, Du Y, Zeng S. Shell cross-linked stearic acid grafted chitosan oligosaccharide self-aggregated micelles for controlled release of paclitaxel. Colloids Surf B Biointerfaces 2006;50:97-103.
28. Tripathi P, Kumar A, Jaina PK, Patel JR. Carbomer gel bearing methotrexate loaded lipid nanocontainers shows improved topical delivery intended for effective management of psoriasis. Int J Biol Macromol 2018;120:1322-34
29. Raza K, Singh B, Singla N, Negi P, Singal P, Katare OP. Nano-lipoidal carriers of isotretinoin with anti-aging potential: Formulation, characterization and biochemical evaluation. J Drug Target 2013;21:435-42.
30. Freag MS, Elnaggar YS, Abdallah OY. Development of novel polymer-stabilized diosmin nanosuspensions: *In vitro* appraisal and *ex vivo* permeation. Int J Pharm 2013;454:462-71.
31. Hu Y, Jiang X, Ding Y, Ge H, Yuan Y, Yang C. Synthesis and characterization of Chitosan-poly(acrylic acid) nanoparticles. Biomaterials 2002;23:3193-201.

Source of Support: Nil. **Conflicts of Interest:** None declared.